Egyptian Journal of Geology

https://egjg.journals.ekb.eg

3D Static Reservoir Modeling: A Case Study from the Early Pliocene Kafr Elsheikh Reservoir, Sapphire Thermogenic Gas Field, Mediterranean, Egypt

Ahmed I. A. Salama[1], Adel A. A. Othman [2], Farouk I. Metwalli[3] and **Mohamed F. Mohamed[2]**

[1]*Exploration department, Egyptian General Petroleum Corporation, Nasr city, Cairo, Egypt*

[2]*Geology department, Al-Azhar University, Nasr city, Cairo, Egypt*

[3]*Geology department, Helwan University, Helwan, Cairo, Egypt*

SAPPHIRE thermogenic gas field is located in the west delta deep marine area, Mediterranean Sea, Egypt. The main hydrocarbon bearing formation is the Early Pliocene Kafr Elsheikh slope channels. The principal purpose of this study is to generate a 3D model able to study the structure framework, facies distribution and petrophysical parameters to understand the reservoir characterization distribution and locate a new prospecting location in the sapphire field. Early Pliocene Kafr Elsheikh slope channels has been subdivided into four members; Sapphir-40,60,70 and 80 channels from top to bottom. Both facies and their petrophysical characteristics have been populated into structure model, which has helped in demonstration of the variation in the reservoir properties, and will help in optimizing the choices for the further exploration and developments.

Keywords: Static reservoir modelling, Structure model, Reservoir characterization, Facies interpretation and Sapphire thermogenic gas field.

1. Introduction

Sapphire Field is one of the largest Pliocene thermogenic gas fields in the Nile Delta, which lies offshore in the deep water (250-1500m) of the present-day Nile delta. The study area is located within west delta deep marine conceasion and covering an area of about 152 km2 (Fig.1). The current research is developed to understanding the subsurface geology of the Sapphire Lower Pliocene field by building accurate modeling of facies, petrophysical and fluid characteristics in three dimensions to identify new locations to drill development wells in the field. Three-dimensional (3D) modeling of subsurface reservoirs is the key factor that controls hydrocarbon reservoir evaluation and simulation for better exploitation and successful development. Although, oil and gas reservoirs can readily be 3D geologically modelled using a variety of software options, but accuracy in the modelling remains a significant barrier. that has a great impact on the effective development of subsurface reservoirs (Abdel-Fattah et al., 2010, Bryant & Flint, 1993, 2009; Radwan, 2022).The main advantage of the ability to accurately simulate complex reservoirs with varying lithologies and reservoir heterogeneities comes from 3D modelling methodologies, and so accurate parameters and the best data integration are required for better reservoir modeling. The geological model allows attributes to be assigned to each cell, and the quantitative reservoir models are often cell-dependent. Such models place far greater challenges on the geologist than conventional models do because geology requires a complete explanation at any point within a reservoir's 3D volume. A 3D geological model can be constructed using many integrated attributes, which is essential for integrating information from a wellbore to a 3D geological model in order to create efficient reservoir simulations (Abdelmaksoud et al., 2019a; Abu Amarah et al. and 2019; Radwan, 2022). The ultimate goal of this study was to provide a new set of potentially optimistic locations for hydrocarbon accumulation and determine the reservoir properties in complex and heterogeneous sapphire slope channels, using accurate 3D modeling to overcome the associated facies changes and reservoir complexity of sapphire slope channels. The reservoir architecture, petrophysical parameters, structural framework, and facies distribution must be understood and recognized. In this work, the grid cells of a 3D model were filled with integrated built (structural modelling), discrete (facies modelling), and continuous attributes (petrophysical modeling). Therefore, we utilized available data from 3D seismic reflection cube and wireline logs to define the main structural characteristics of the study area, recognize distribution of thickness/facies of sapphire slope channels reservoir and evaluate its petrophysical properties

2Geologic Setting

The Nile Delta province is an example of a passive edge sedimentary basin that was created by thermal

*Corresponding author e-mail:ahmed.abosalama.850@gmail.com
Received: 10/02/2023; Accepted: 07/04/2023
DOI: 10.21608/EGJG.2023.191277.1036

subsidence after the Afro-Arabian plate was severed by extensional tectonics from the Eurasian plate through the Late Triassic-Early Cretaceous time (May, 1991). The Nile Delta has a sediment pile several kilometres thick that consist of clastic sediments formed during a series of Tertiary delta progradations separated by flooding events. (Fig.2) shows the stratigraphic column of the Nile Delta, highlighting the study interval. A system of NE- trending fold axis was generated as a result of Rosetta and Temsah transgressive movements during the Early–Middle Miocene (Farouk et al. 2021). The Sapphire thermogenic gas field is located within the West Delta Deep Marine area that covers an area of about 152 km2 (Fig.1). Sapphire field is associated with NDOA (Nile Delta offshore Anticline) that take ENE direction that is parallel to the NE Rosetta fault trend (Fig.3,4,5,6 and Fig.7). The reservoir target within our area is deep marine basin floor fans and base of slope channel sands concentrated within the Kafr El Sheikh formation towards the base of the Pliocene (Fig.2).

3Workflow and Results

There are four steps involved in building the 3D geo-cellular model of the sapphire thermogenic gas field. (Fig.2): data preparation, data interpretation, structure modeling, distribution of the facies and petrophysical properties within the 3D model

3.1Data Preparation

Sapphire-3, Sapphire-dd, Sapphire-de, Sapphire-deep-1, Sapphire-dq, Sapphire-SC-1, and Sapphire-SW-1 wells were the seven input wells used to create a more detailed sapphire field model. well headers, directional survey, formation tops, wireline logs and petrophysical logs (V-shale, effective porosity and water saturation), 3D post stack seismic cube (Sapphire Deep Seismic-2010), fault sticks data supplied from seismic interpretation, depth structure contour maps. seven faults and five horizons (sapphire-40, 60, 70, 80 and Messenia, Fig. 4,5,6,7 and 8) have been interpreted and selected for this model.

3.2Data Interpretation

After the data is prepared, the data analysis is done using software programs, such as Petrel (@ Schlumberger, 2017), Tech-Log (@ Schlumberger, 2015). As mentioned above the petrophysical analysis was done Tech-Log (@ Schlumberger, 2015). In this part the hydrocarbon bearing units were investigated and petrophysical parameters such as net reservoir, shale content, effective porosity, water saturation was calculated and then introduces into the static model. For example, the table (1) shows the petrophysical properties of Sapphire-80 channel (the main reservoir in the study area), that shows that this channel has very good petrophysical properties where the average reservoir thickness is 16m, average effective porosity is 28%, average shale volume is 24% and average water saturation is 36, then the average of hydrocarbon saturation is 64%. In this part horizon and fault interpretation were done for five levels (sapphire-40, 60, 70, 80 and Messenia, Fig. 4,5,6,7 and 8). The trapping mechanism includes up-dip fault seal against the NDOA fault to the north and dip closure to the south, the channel sands have stratigraphical closure with pinch-out to the east and west.

3.3Structural Model

Reconstructing the structural properties of the reservoir, by defining a set of faults running through it. The Sapphire field structural model (Fig.10) was the first stage to make the complete model. The model was based on the depth converted 3D post stack seismic data (Sapphire Deep Seismic-2010). Input data consist of fault sticks of interpreted faults. Fault modeling (Fig.9), Subsequently horizons, zones and layers can be inserted into it. As is shown in the (Fig. 4,5,6,7,8 and 9). The reservoirs are faulted by 8 faults that are related to tension movement in upper early Pliocene age (Sehim el at 2002), and takes three trends (ENE-WSW, NE-SW, and N-S), all faults are normal faults (extensional faults), 1-Fault with N-S trend, 5-Faults with ENE-WSW trend, 2-Faults with NW-SE trend, the displacement on the man fault is toward the southeast, the ENE-WSW is the main trend in the study area which dissect ENE-SSE NDOA (Nile delta offshore anticline) which generated as a result of Rosetta and Temsah transgressive movements during the Early–Middle Miocene along which three-way dip closure was developed. Once the fault model network and gridding are built the Sapphire-40, Sapphire-60, Sapphire-70, Sapphire-80 and Messinian (Fig. 4,5,6,7 and Fig. 8) horizons are constructed from depth seismic data and then inserted into 3D grid as the first step in stratigraphic subdivision of the model. Thus, the structural model has been built by these horizons. Finally, all the fault segments and picked horizons were inserted in 3D structure model (Fig.10), by making horizon process, then these horizons were divided into number of layers in order to increase the vertical resolution of the layers while running the property modeling.

3.4 Upscaling

After Structural modeling and before facies modelling, scale up well logs should be done. Before the data distribution across the model, the source of these data is obtained from well log values was necessary to be assigned to the cells penetrated by the wells. This

process in Petrel software known as scale up well logs, the upscaled logs used to fill up the 3D grid with properties. Scaling up is inserting the value of cells that are penetrating by wells. Each cell must have one value, so well property must be averaged, this step uses well parameter as an input, where you resample the log data representing each well at the cells penetrated by those wells. process can be concluded by the log values to the cell and distribute this property into 3D grid. In the present study, the key input is the interpreted well logs of chosen wells in this upscaling and the chosen method for the upscaling is the averaging method. the facies log is generated based on other logs such as gamma ray, bulk density, sonic, etc. The arithmetic mean is used as an averaging method in the upscaling of the continuous petrophysical property logs (porosity and water saturation) of Sapphire reservoir. Before going further with the model, the results of scale up facies and rock properties have been checked to make sure that the main heterogeneities that influence flow are preserved after scale up the logs. upscaled logs for facies, porosity and water saturation of sapphire field are shown in Figs. (11-13) respectively. After scale up the lithofacies, effective porosity and water saturation within the wells, the next stage is to populate all cells in the model with these properties.

3.5 Facies Modelling

Facies modelling is the interpolation of discrete data such as facies throughout the 3D model or estimating the field's distribution of reservoir facies change. Classification of facies and their accurate representation in a 3D cellular geologic model is critical because permeability and fluid saturations for a given porosity vary considerably among facies (Dubois et al., 2003). In the current research, Upscaled facies logs are employed in the modelling of faces process and the stochastic sequential indicator simulation (SIS), which is one of the techniques primarily utilized for categorical data like facies, is employed in the facies modelling of the reservoir. the final result shown in fig. (14a, 15a, 16a, 17a, 18a and 19a), where facies maps and cross sections derived from model of sapphire channels (lower part of Kafr Elsheikh formation).

3.6 Petrophysical Modelling

One of the main aims of static model is to show reservoir parameters (porosity, permeability and water saturation) extension in three dimensions, petrophysical model depends on the evaluation of wireline-logs. Petrophysical parameters change is function of facies change. Commonly it is used in combination with facies modelling to capture geological heterogeneity at different scales. petrophysics is typically one or two dimensional. The 3D distribution of petrophysical properties is based only on the vertical well profiles. Sequential Gaussian Simulation algorithm is used as a statistical method which fits with the amount of the available data. With the same procedures for the facies modelling, the petrophysical modelling was made, the main inputs required for petrophysical modelling process are the upscaled well logs (Effective porosity and Water saturation). The distribution of the facies and petrophysicalparameters in the current study well be clarify in the following section.

3.6.1 Sapphire-40

Sapphire-40 channel is located at the top of the interval under study, As is shown in the facies maps figure (14a), there are three facies in this level: shale, sandstone and siltstone. the main trend of sapphire-40 is NNW-SSE runs across the area and is cutting by many faults among these faults, the major one (ENE-WSW) which compartmentalize the field into two parts, the channel become wide near this fault and dominated by sand while become thinner and dominated by silt that graduated to shale away from this fault near the borders of the study area that indicate that this fault effects on the deposition of the sapphire-40 facies. As well as the final result for petrophysical modelling of sapphire channel-40 are shown in figure (14b and c), for effective porosity as shown in figure (14b), its value ranges between 10-30% in sapphire channel, and it is increase around the main fault in central part of the study area and decrease away from it where the shale is dominated. For the water saturation as shown in figure (14c), its value ranges between 10-90% in sapphire 40, and it is increase around the main fault (ENE-WSW trend) in central part of the study area where the main trap of sapphire channels and decrease away from it. As well as the cross sections from facies and property model used and show the reservoir heterogeneity clearly, as is shown in figures (17a, b and c) and (18a, b and c). figure (17a, b and c): E-W cross section figures (17a) shows spreading of different facies across the field where at the top part (sapphire-40) is dominated by five separate branches of sapphire-40 channel dominated by sand facies intercalated with layers of shale and minor percentage of siltstone. While the N-S cross sections (18a), shows the same facies and also show the sand is restricted to southern and central parts of the study area around the main fault ENE-WSW trend and gradually changed to the shale facies to the north. As shown in the figures (18a,b, c and 19a,b, c): the lateral and vertical changing of the different petrophysical parameters (effective porosity and water

saturation) is found to be directly related to lateral and vertical facies changes

3.6.2 Sapphire-60

Sapphire-60 is located in the middle part of the studied interval, As is shown in facies maps figure (15a), there are three facies in this level: shale, sandstone and siltstone. sapphire-60 is limited in its extension to eastern region at upthrown side of the study area around the main fault, the channel become wide near this fault and dominated by sand while become thinner away from the main fault and gradually changed to shale facies that indicate that this fault effects on the deposition of the sapphire-60 facies. As well as the final result for petrophysical modelling of sapphire channel-60 exhibited in figures (15b and 15c), for effective porosity as demonstrated in (figure 7-8b), its value varies between 10-25%, and it is increase around the main fault in central region of the study area and decrease away from it where the shale is dominated. In regards to the water saturation depicted in figure (15c), its value varies between 10-80%, and it is increase around the main fault (ENE-WSW trend). As well as the cross sections from facies and property model used and show the reservoir heterogeneity clearly, figures (18a, b, c and 19a, b, c): E-W cross section figure (18a) shows spreading of different facies across the field where at the middle part (sapphire-60), where the sand is restricted to the eastern region and intercalated with layers of shale and minor percentage of siltstone, while toward the western part the reservoir facies are changed to pure shale facies. N-S cross sections (18ab) shows that the middle part of the studied interval is pure shale. As shown in the figures (18a,b, c and 19a,b, c): the lateral and vertical changing of the different petrophysical parameters (effective porosity and water saturation) is found to be directly related to vertical and lateral facies changes

3.6.3 Sapphire-70

Sapphire-70 is located in the middle of the studied interval, As is shown in the facies maps figure (16a), there are three facies in this level: shale, sandstone and siltstone. sapphire-70 is limited in its distribution in central parts of the study area along the main fault, the channel become wide near this fault and dominated by sand while become thinner away from the main fault and gradually changed to shale facies that indicate that this fault effects on the deposition of the sapphire-70 facies. As well as the final result for petrophysical modelling of sapphire channel-70 exhibited in figures (16b and c), for effective porosity as shown in (figure 16b), its value varies between 8-30%, and it is increase around the main fault in central part of the study area and decrease away from it where the shale is dominated. For the water saturation as shown in (figure 16c), its value ranges between 40-80%, and it is increase around the main fault (ENE-WSW trend). As well as the cross sections from facies and property model used and show the reservoir heterogeneity clearly, figures (18a, b, c and 19a, b, c): E-W cross section figure (18a) shows spreading of different facies across the field where at the middle part (sapphire-70), where the sand is restricted to the eastern and western parts and intercalated with layers of shale, from the petrophysical analysis overview the average of shale volume in sapphire-60 is 24%, while in the central part the reservoir facie are changed to pure shale facies. N-S cross section (19a) shows that the middle part of the studied interval is pure shale. As shown in the figures (18a,b, c and 19a,b, c): the lateral and vertical changing of the different petrophysical parameters (effective porosity and water saturation) is found to be directly related to vertical and lateral facies changes

3.6.4 Sapphire-80

Sapphire-80 is located in the lower part of the lower Pliocene, As is shown in the facies maps figure (17a), there are three facies in this level: shale, sandstone and siltstone. the main trend of sapphire-80 is NNW-SSE runs across the area and is cutting by many faults among these faults the major one (ENE-WSW) which compartmentalize the field into two parts, the channel is distributed continuously from east to west on both sides of the main fault (NNW-SSE) and branches in small channels toward NWN direction. As well as the final result for petrophysical modelling of sapphire channel-80 are shown in figure (17b and 17c), for effective porosity as shown in (figure 17b), its value varies between 8-35%. For the water saturation as shown in (figure 17c), its value varies between 10-80%, and it is increase around the main fault (ENE-WSW trend). As well as the cross sections from facies and property model used and show the reservoir heterogeneity clearly, figures (18a, b, c and 19a, b, c): E-W cross section figure (18a) shows spreading of different facies across the field where at the lower part (sapphire-80), where the sand facies is found in all area from ENE to WSW and intercalated with layers of shale. N-S cross sections (19a) shows the same facies and also shows that the sand is restricted to southern and central parts of the study area around the main fault ENE-WSW trend) and gradually changed to the shale facies to the north and most south. As shown in the figures (18a,b, c and 19a,b, c): the lateral and vertical changing of the different petrophysical parameters (effective porosity and water saturation) is found to be directly related to lateral and vertical facies changes.

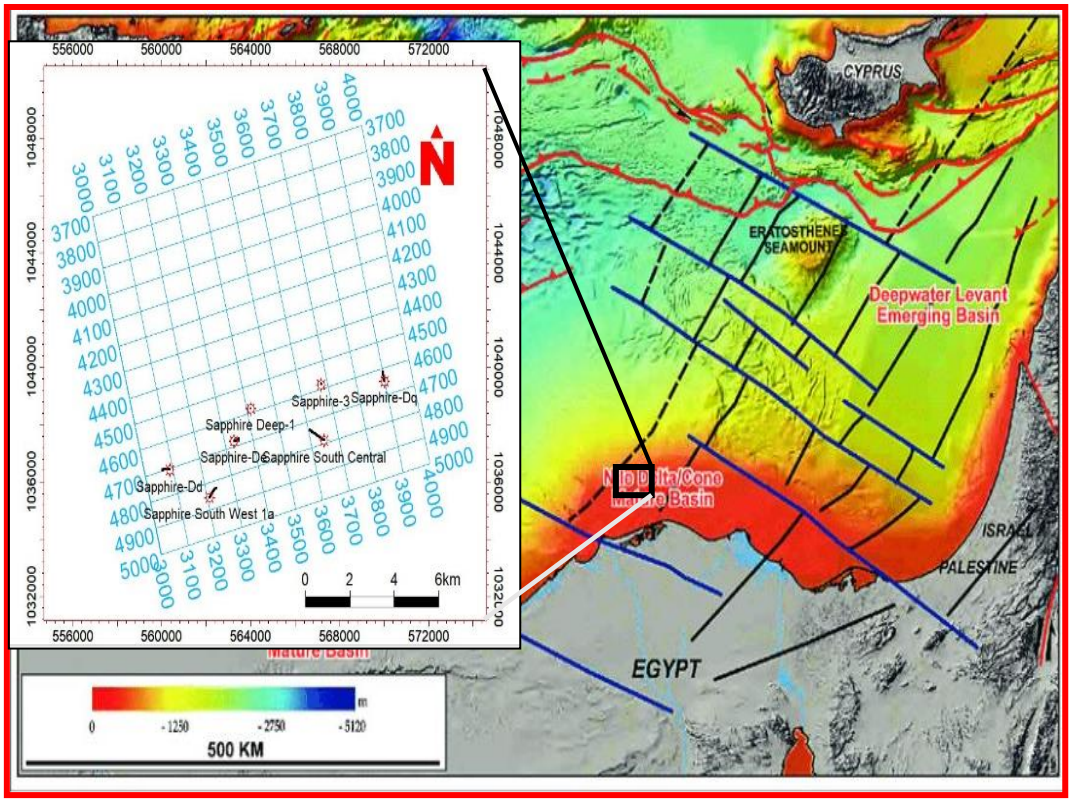

Fig. 1. Location map of the Sapphire Field, selected wells and seismic Cube.

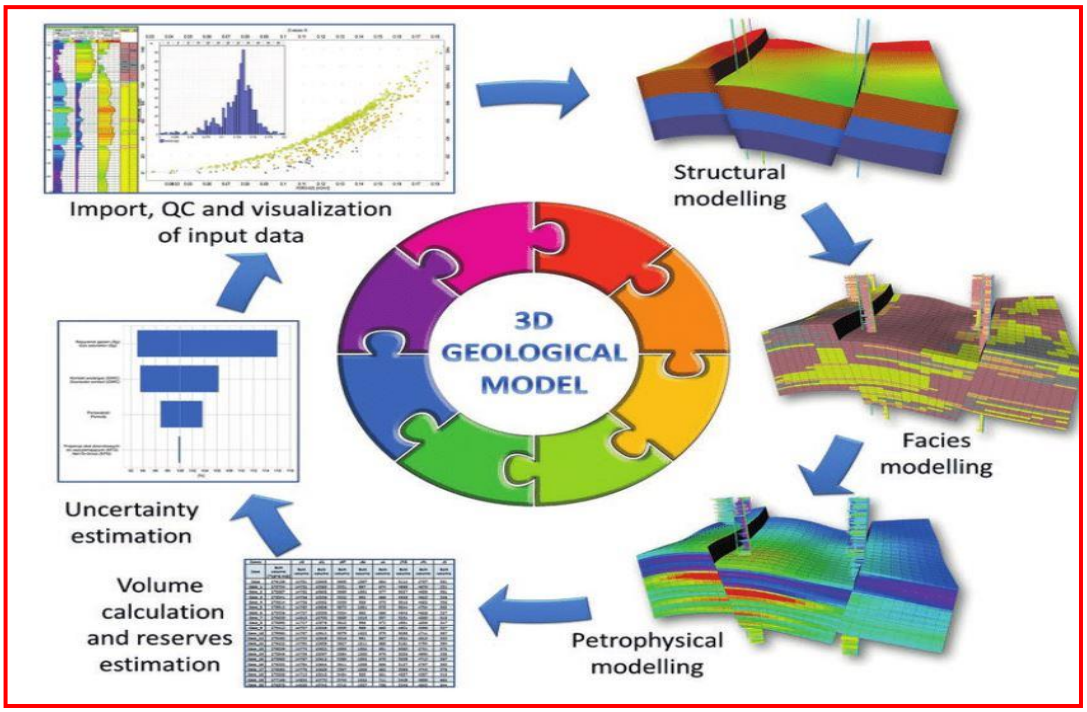

Fig. 2. Main phases of static modelling.

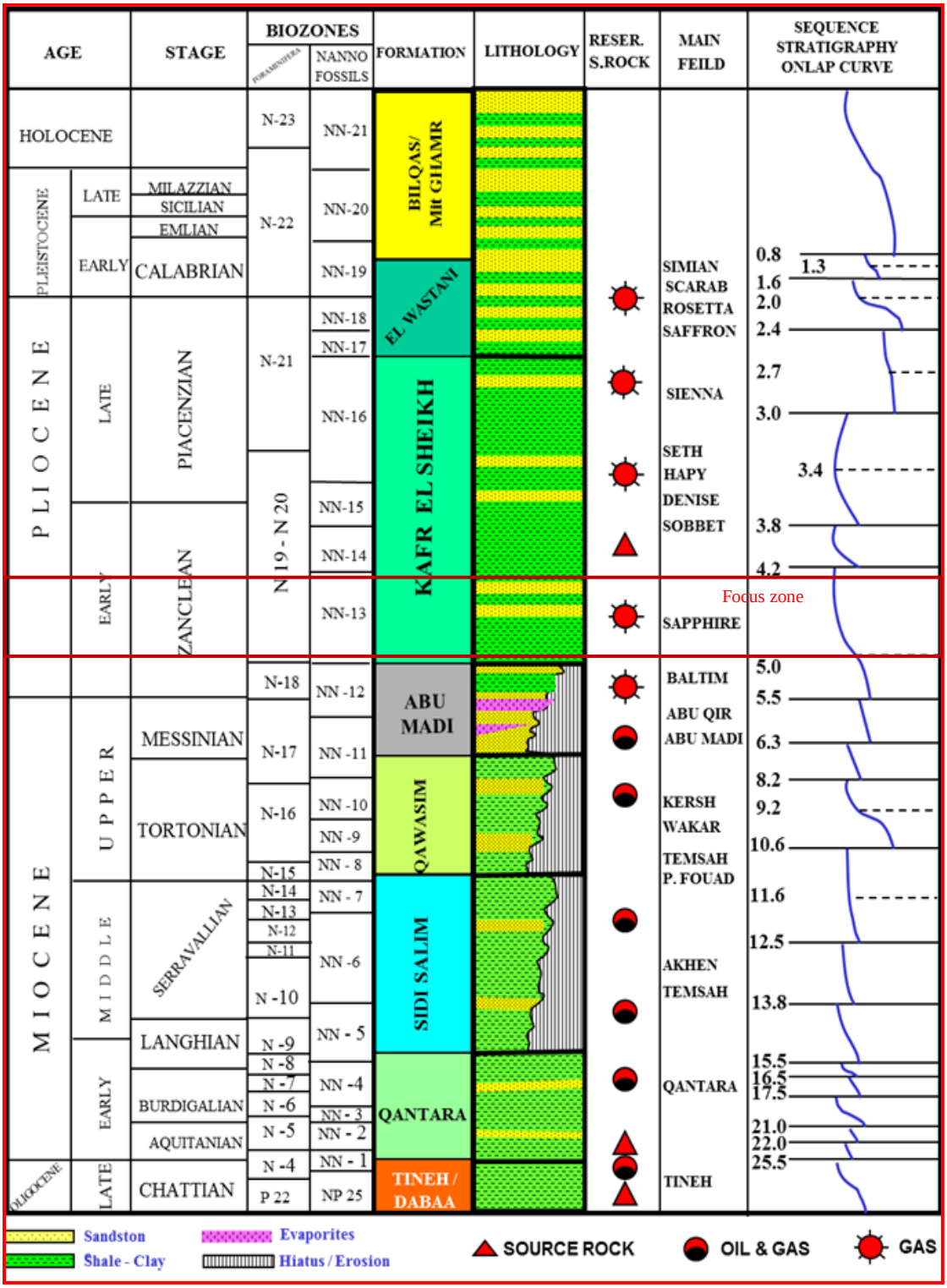

Fig. 3. Nile Delta stratigraphic column and hydrocarbon system. Modified from Rio et al, (1991). showing the study interval.

Table 1. The petrophysical characteristics of the sapphire-80. channel.

Well	*Gross thickness (m)*	*Reservoir thickness (m)*	*Porosity (%)*	*Volume of clay (%)*	*Water saturation (%)*
Sapphire-3	**87**	**21**	**22.5**	**29**	**33**
Sapphire-dd	**50**	**7**	**26**	**23**	**47**
Sapphire-de	**31**	**19**	**29**	**22**	**18**
Sapphire-deep-1	**75**	**29**	**31**	**15**	**31**
Sapphire-dq	**47**	**8**	**28**	**31**	**62**
Sapphire-SC-1	**107**	**13**	**26**	**24**	**30**
Average	**66**	**16**	**27**	**24**	**36**

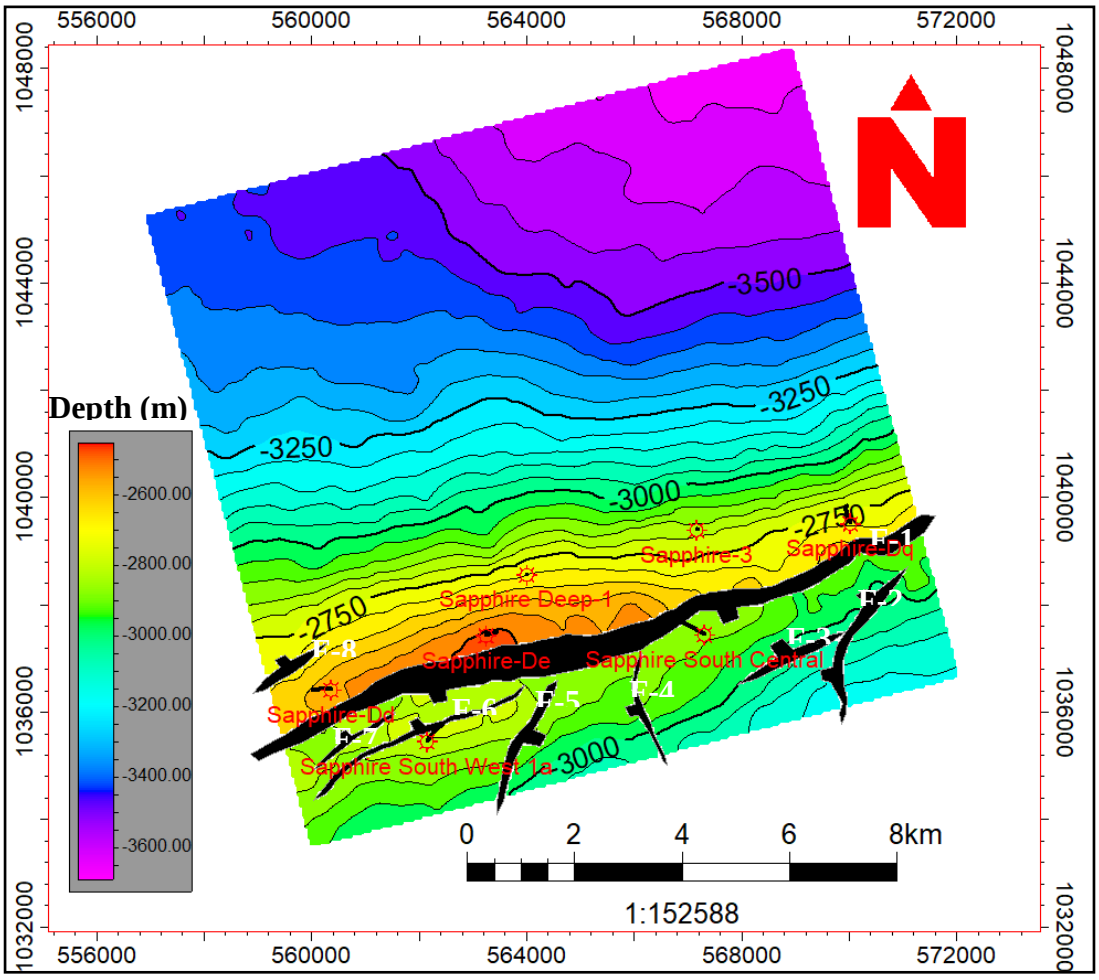

Fig. 4. Depth structure contour map, top Messinian in Sapphire field, showing ENE-WSW NDOA is dissected by three fault trends (ENE-WSW, NE-SW and N-S).

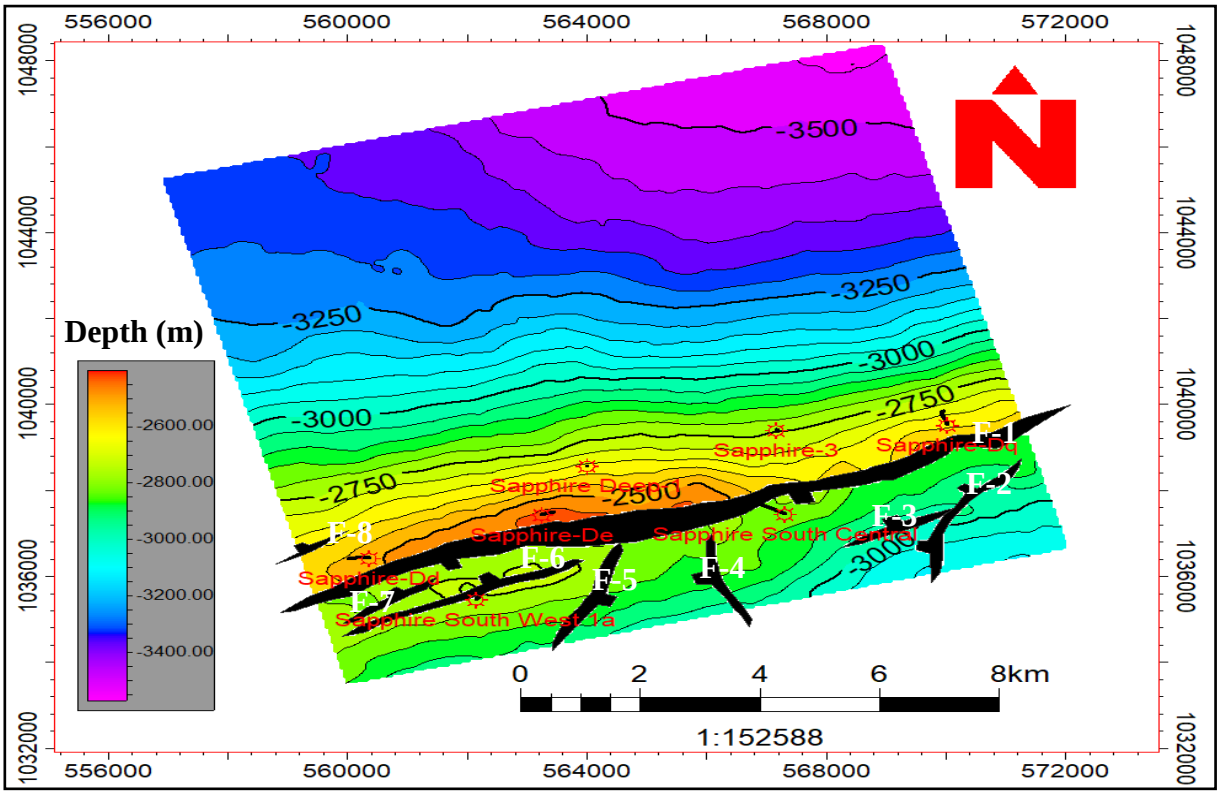

Fig. 5. Depth structure contour map, top Sapphire-80 in Sapphire field, showing ENE-WSW trending NDOA is dissected by three normal fault trends (ENE-WSW, NE-SW and N-S).

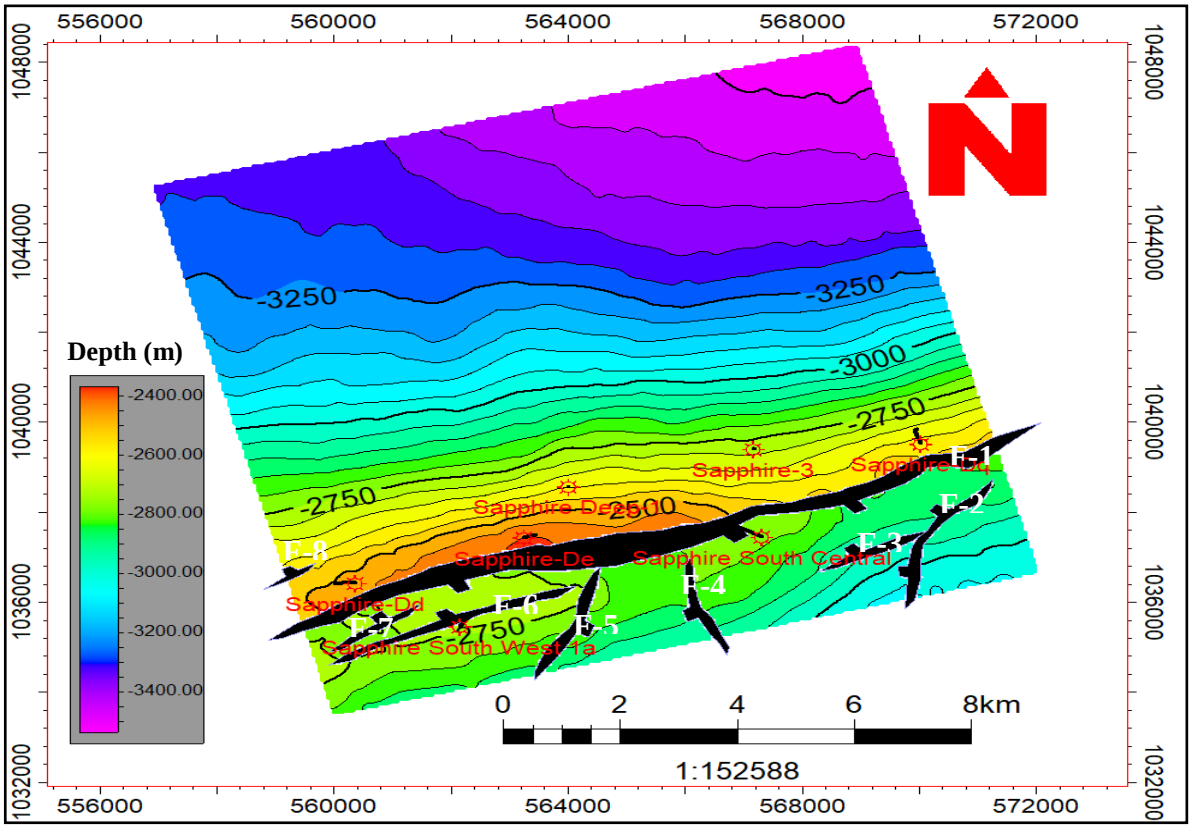

Fig. 6. Depth structure contour map, top Sapphire-70 in Sapphire field, showing ENE-WSW NDOA is dissected by three fault trends (ENE-WSW, NE-SW and N-S).

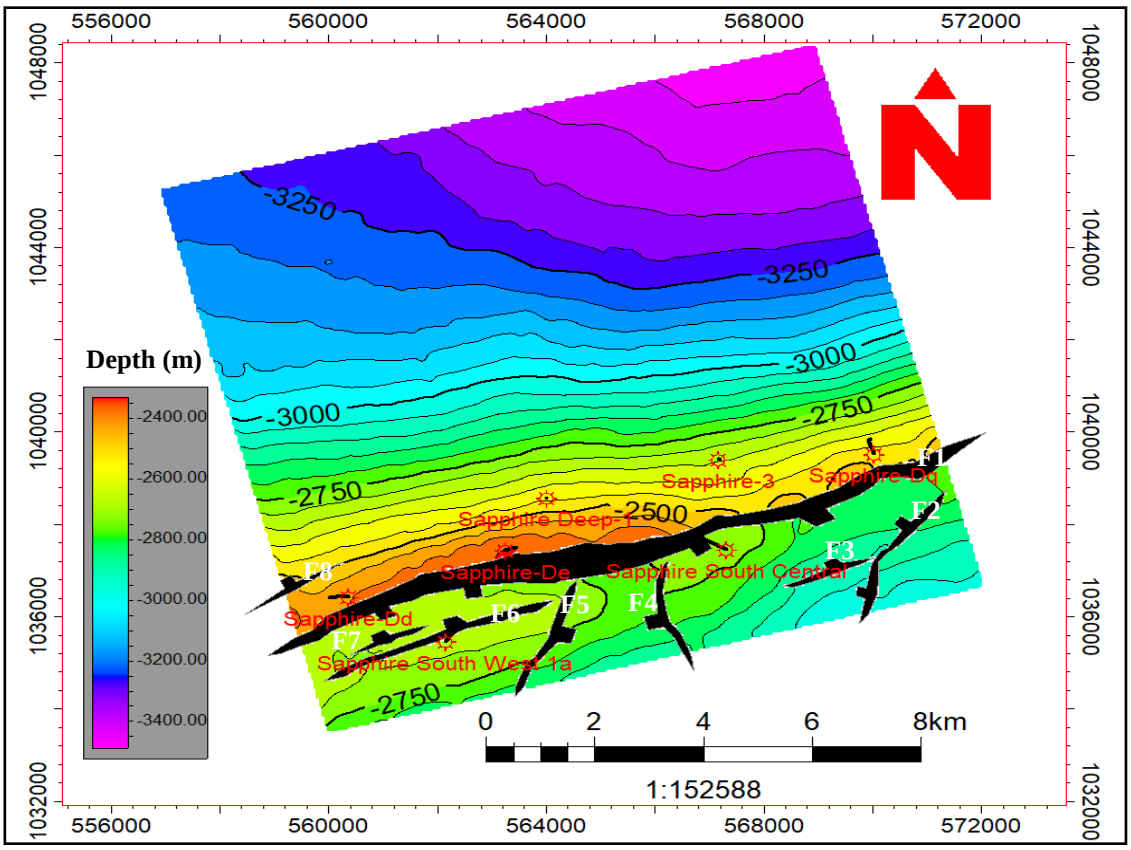

Fig. 7. Depth structure contour map, top Sapphire-60 in Sapphire field, showing the same structural setting as Sapphire-40: ENE-WSW NDOA that is dissected by three fault trends (ENE-WSW, NE-SW and N-S).

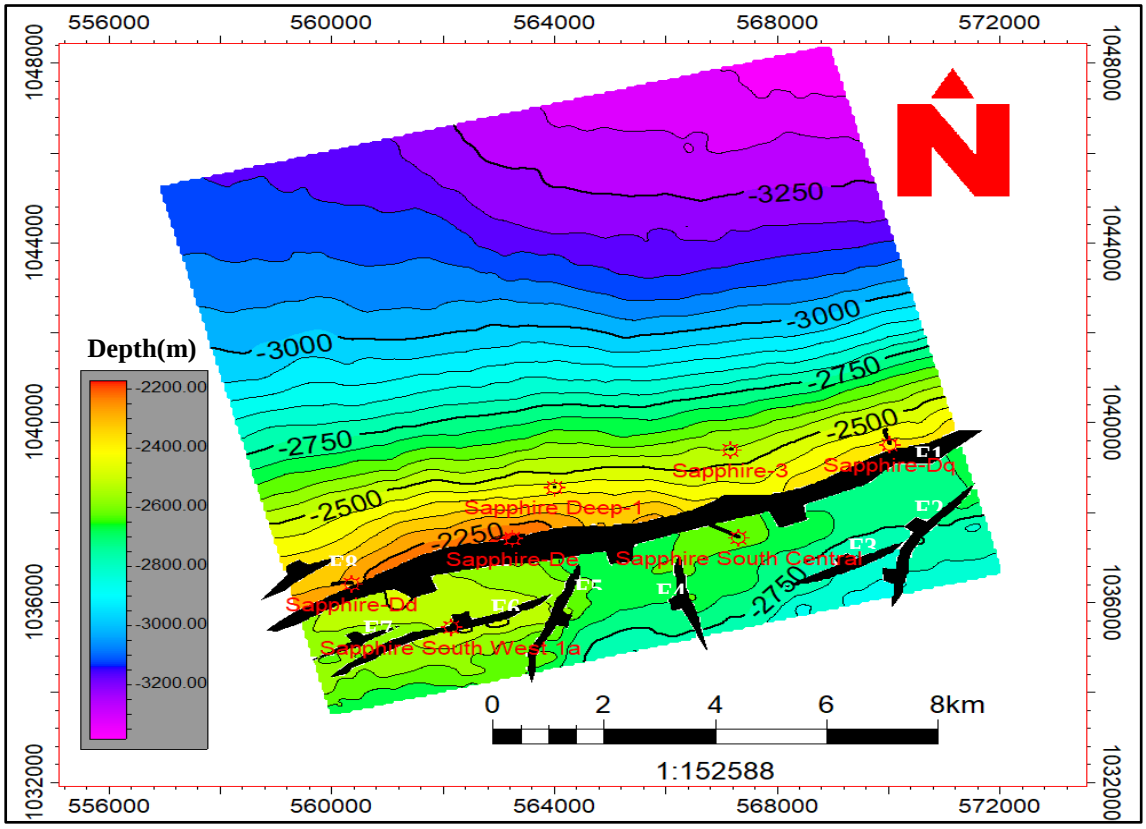

Fig. 8. Depth structure contour map, top Sapphire-40 in Sapphire field, showing ENE-WSW NDOA that is dissected by three fault trends (ENE-WSW, NE-SW and N-S).

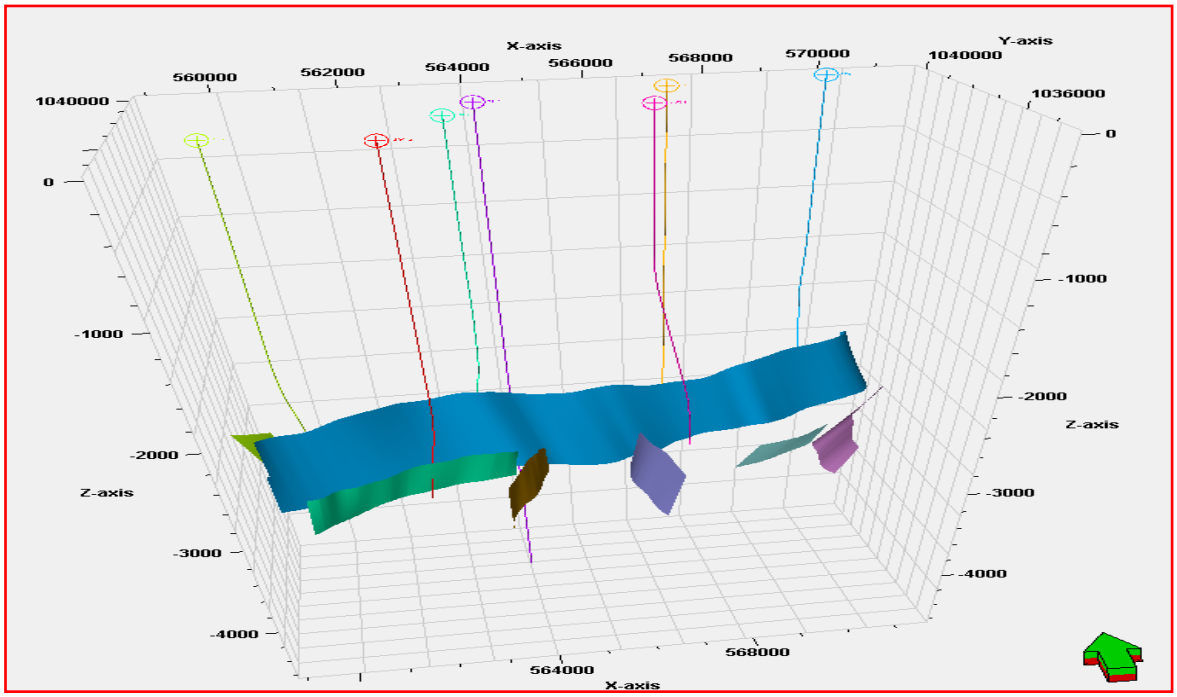

Fig. 9. 3D structural model of sapphire field showing fault modeling.

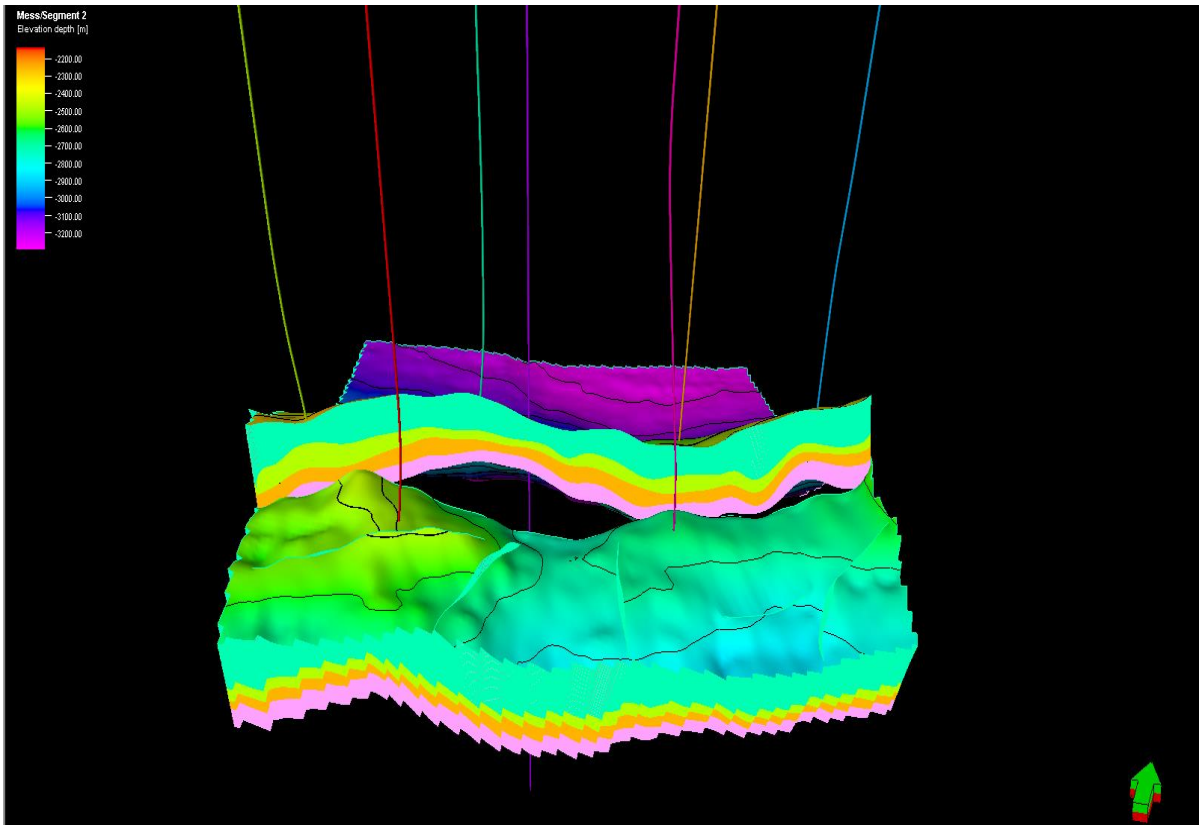

Fig. 10. 3D Structure model of sapphire field showing horizons, zones and faults.

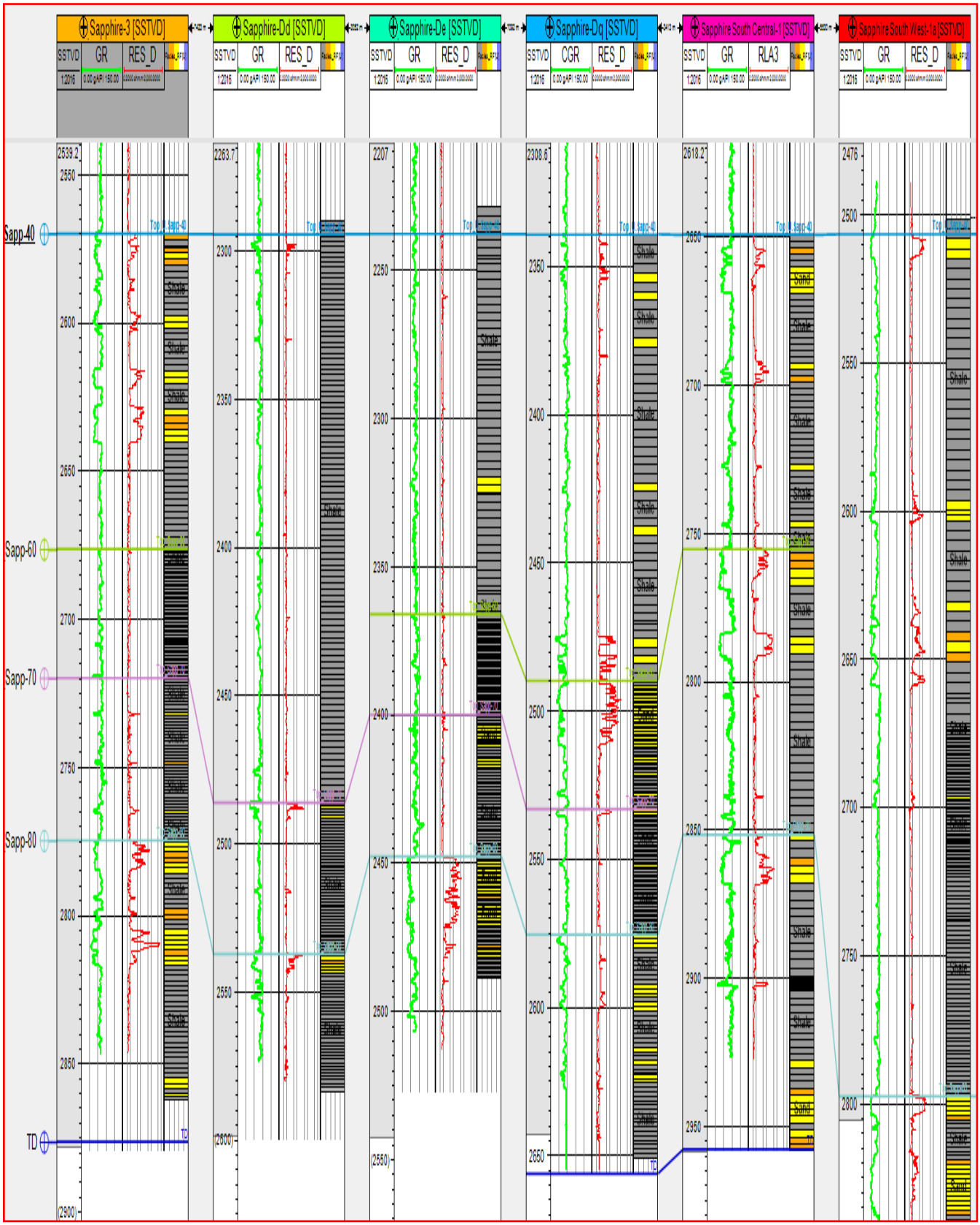

Fig. 11. Facies Upscaling Process for six wells in the study area.

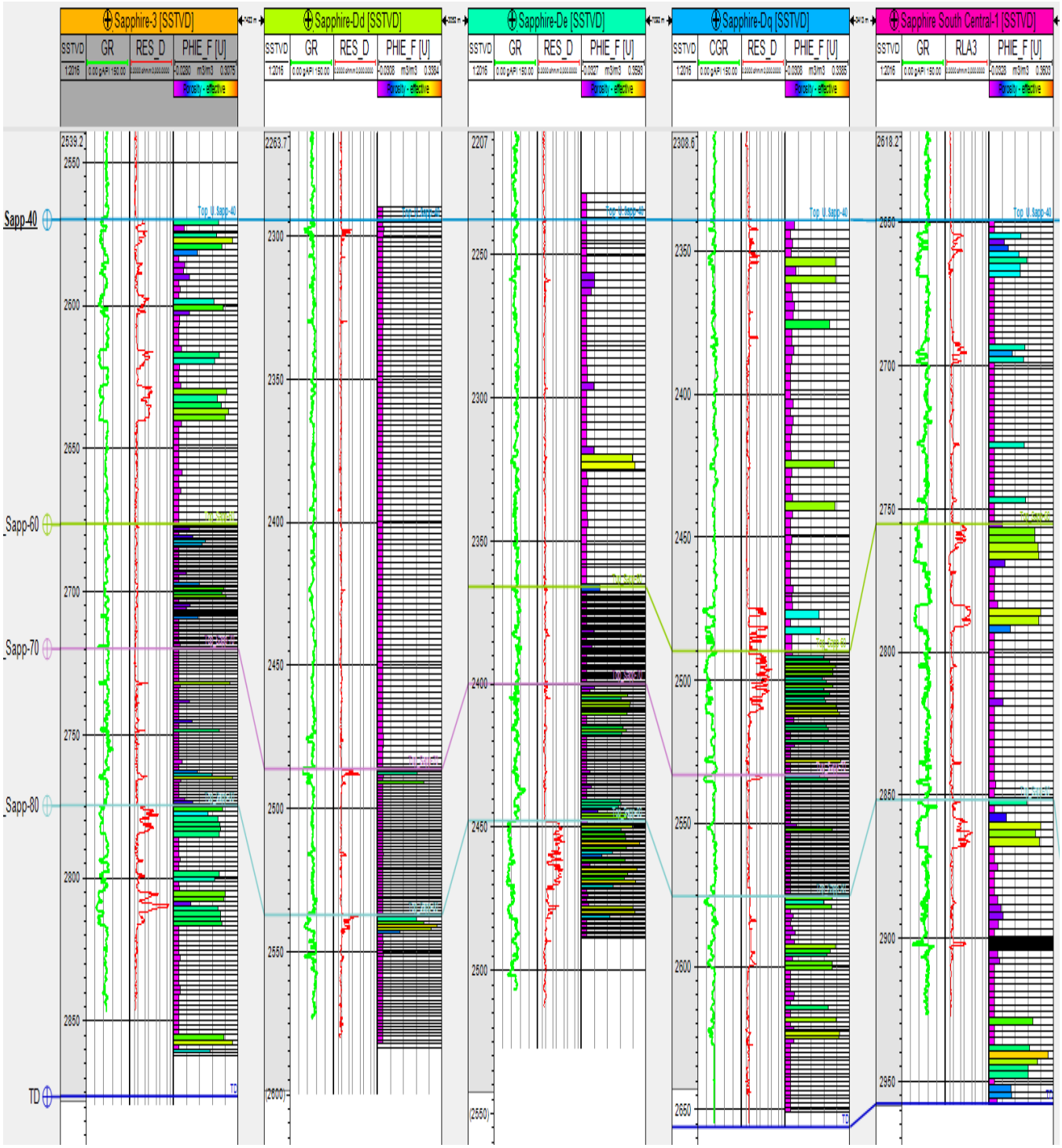

Fig. 12. Facies Upscaling Process for five wells in the study area.

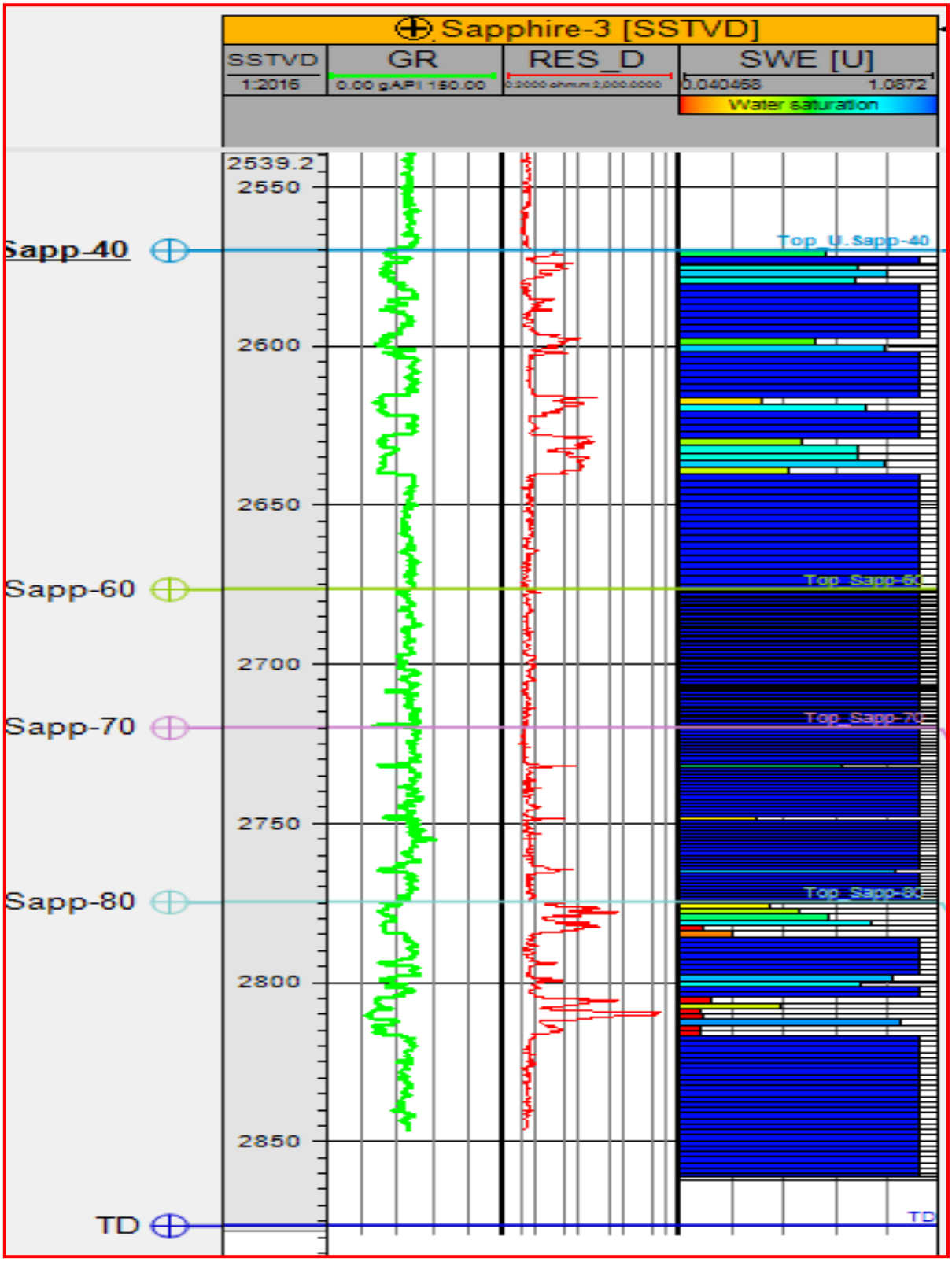

Fig. 13. Facies Upscaling Process for sapphire-3 well in the study area.

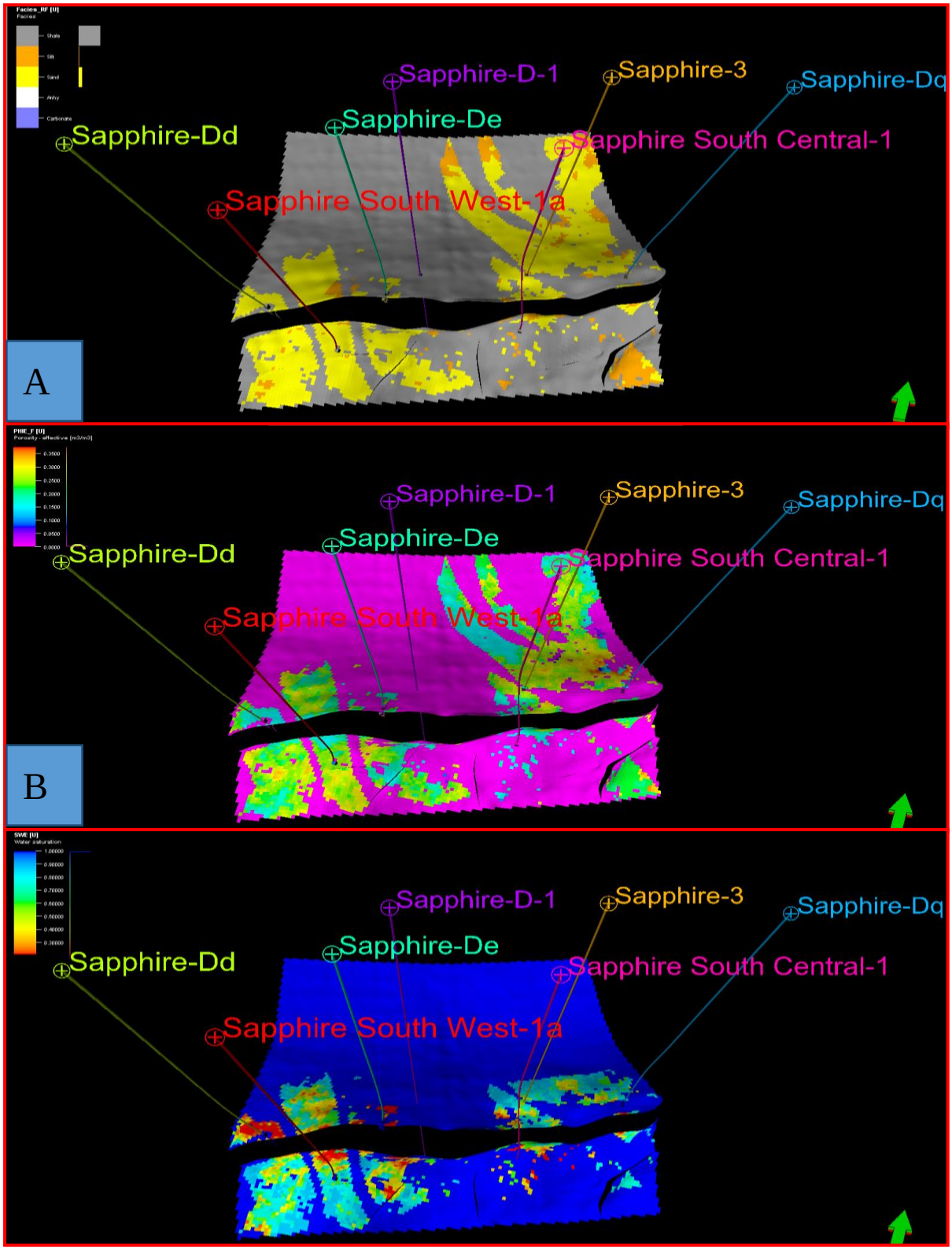

Fig. 14. (a) 3D modelled facies, (b) effective porosity and (c) water saturation Sapphire-40 reservoir.

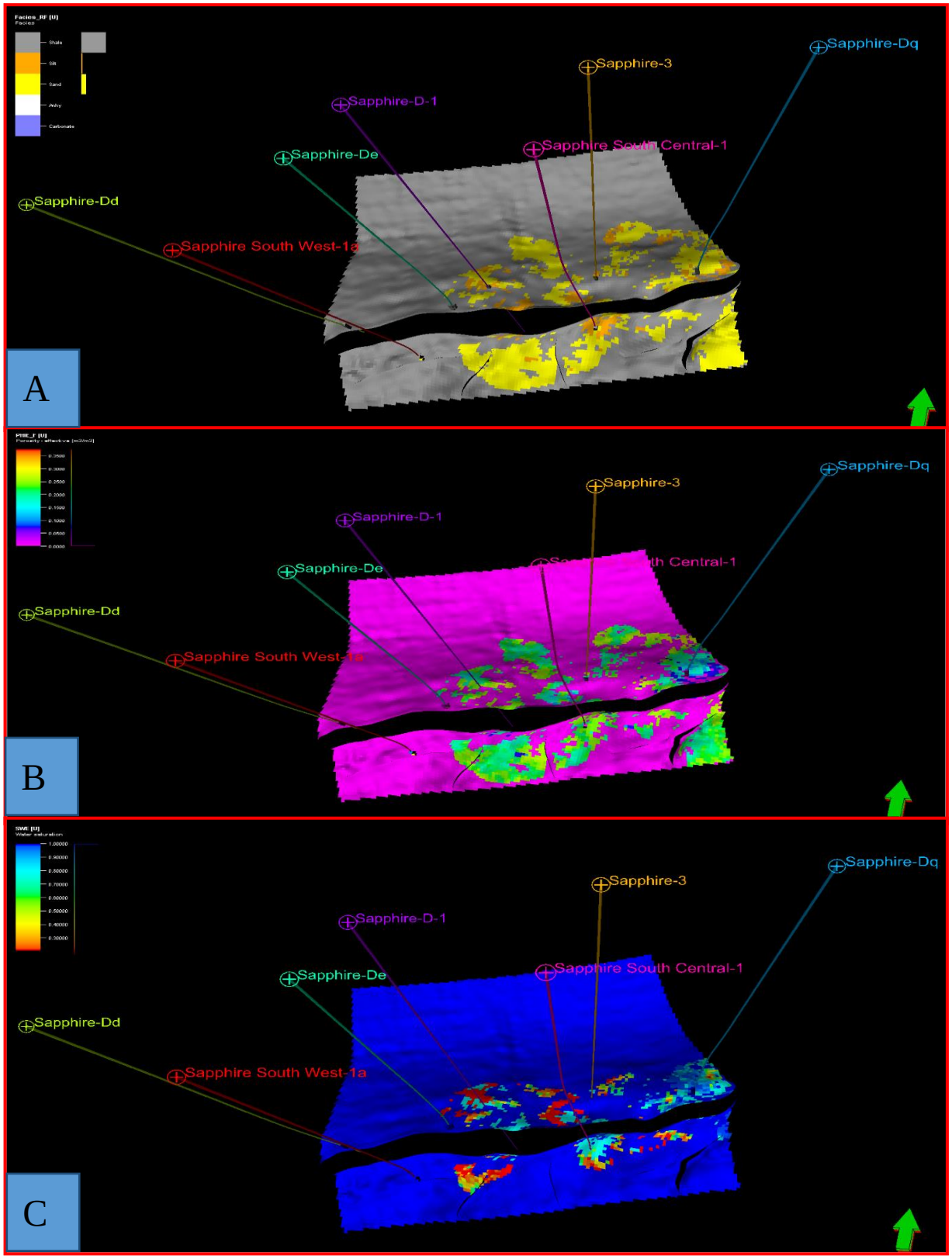

Fig. 15. (a) 3D modelled facies, (b) effective porosity and (c) water saturation Sapphire-60 reservoir.

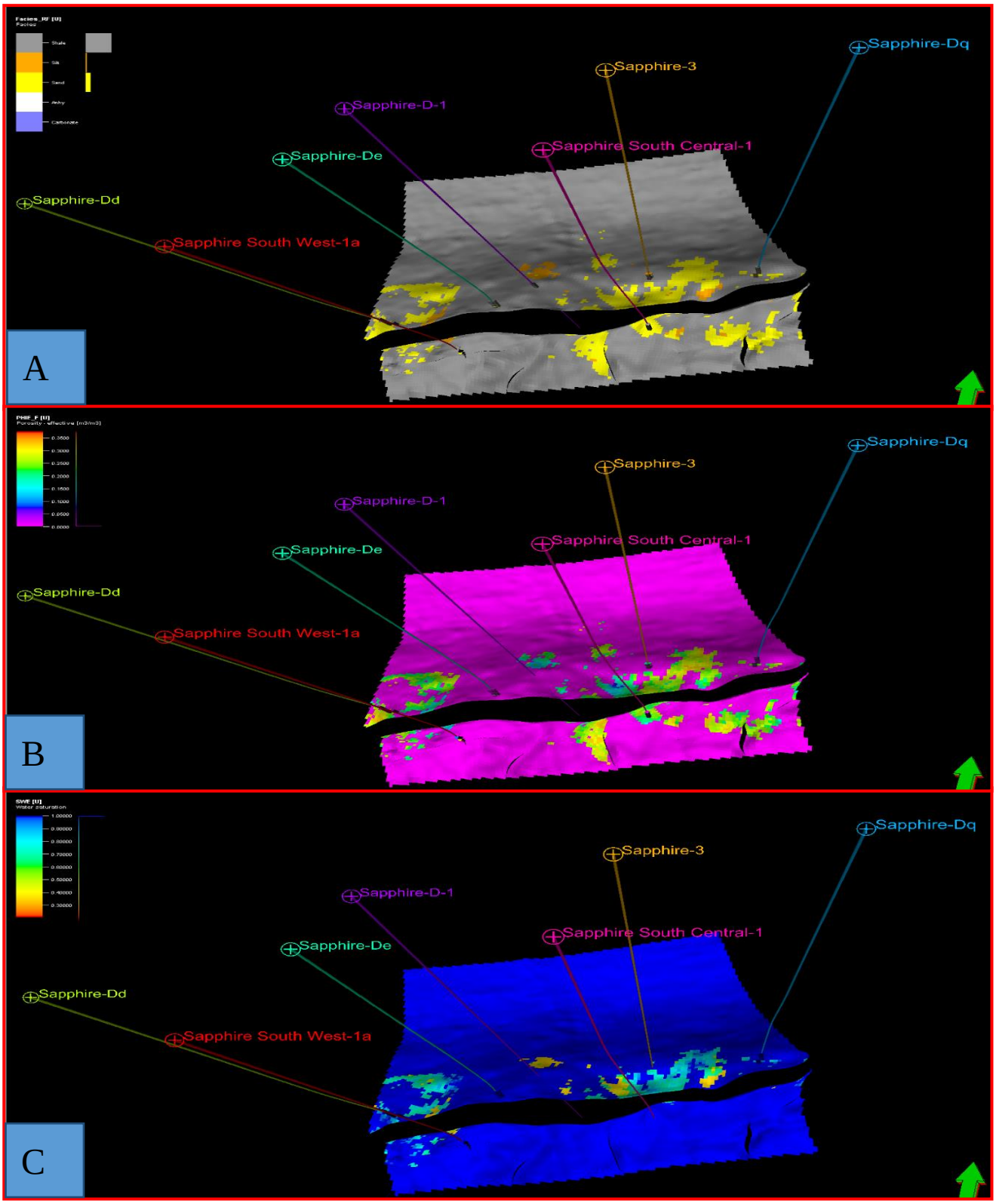

Fig. 16. (a) 3D modelled facies, (b) effective porosity and (c) water saturation Sapphire-70 reservoir.

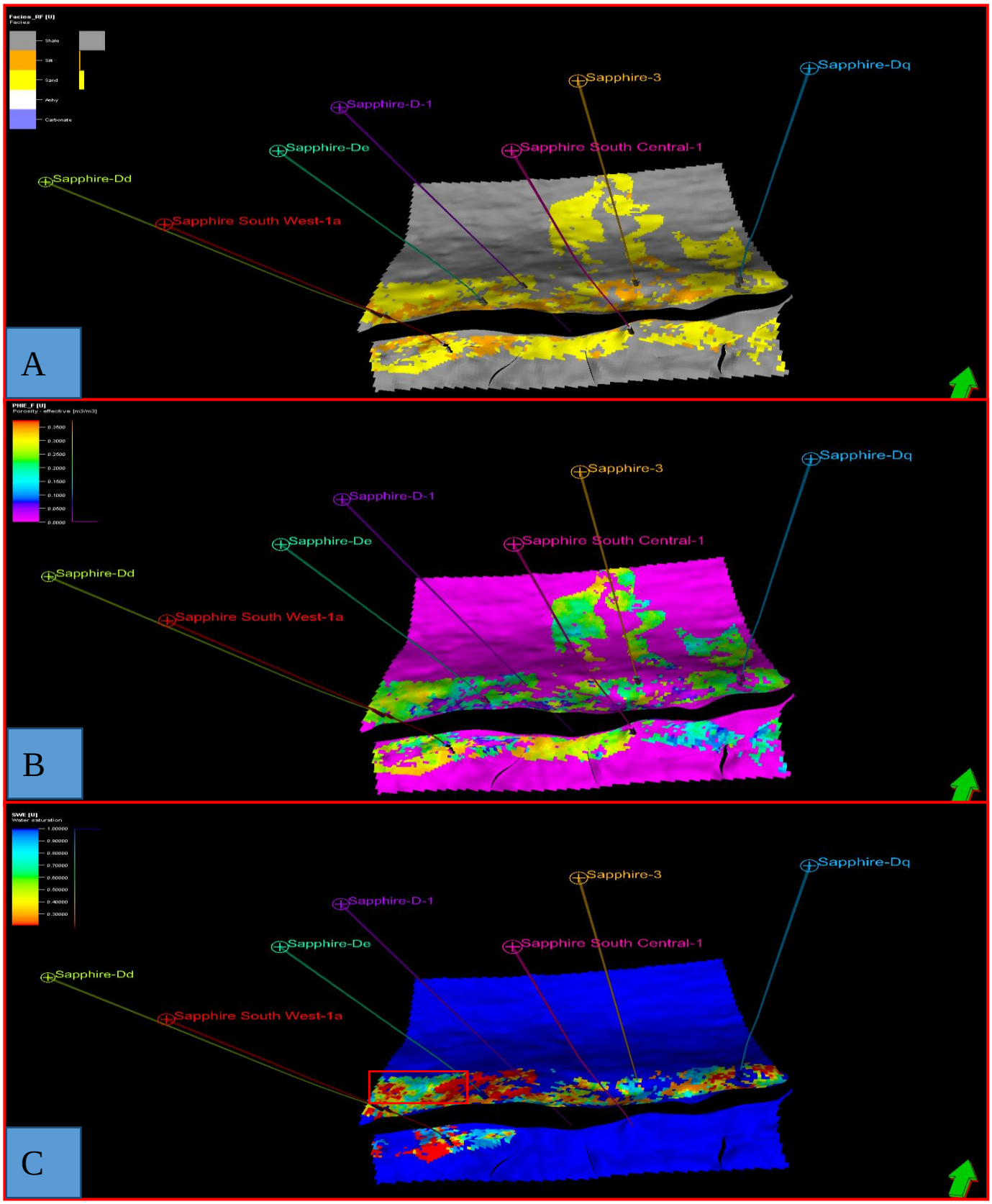

Fig. 17. (a) 3D modelled facies, (b) effective porosity and (c) water saturation Sapphire-80 reservoir.

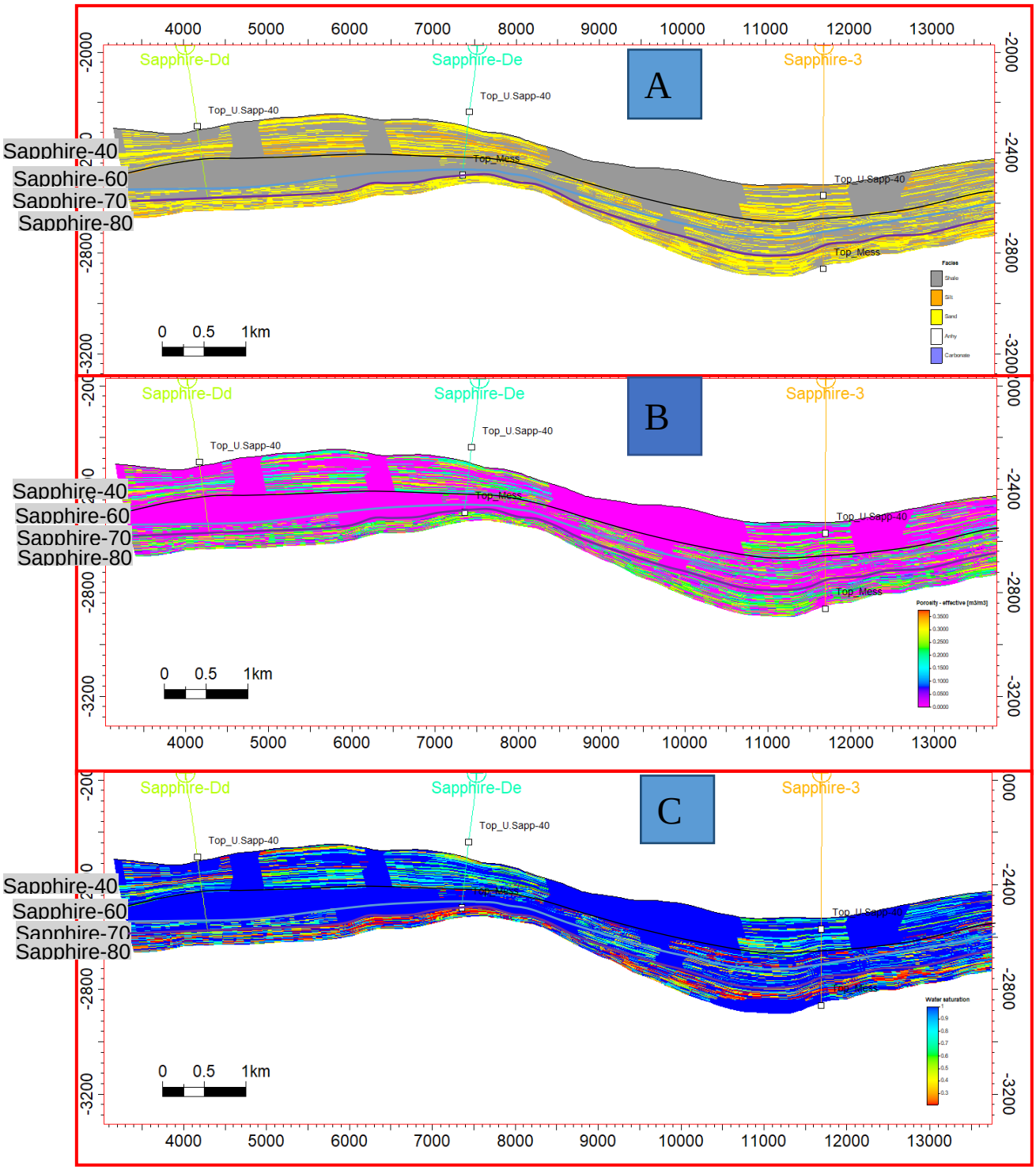

Fig. 18. East-West cross-section through the 3D model: (a) lithofacies, (b) effective porosity and (c) water saturation of the Sapphire field.

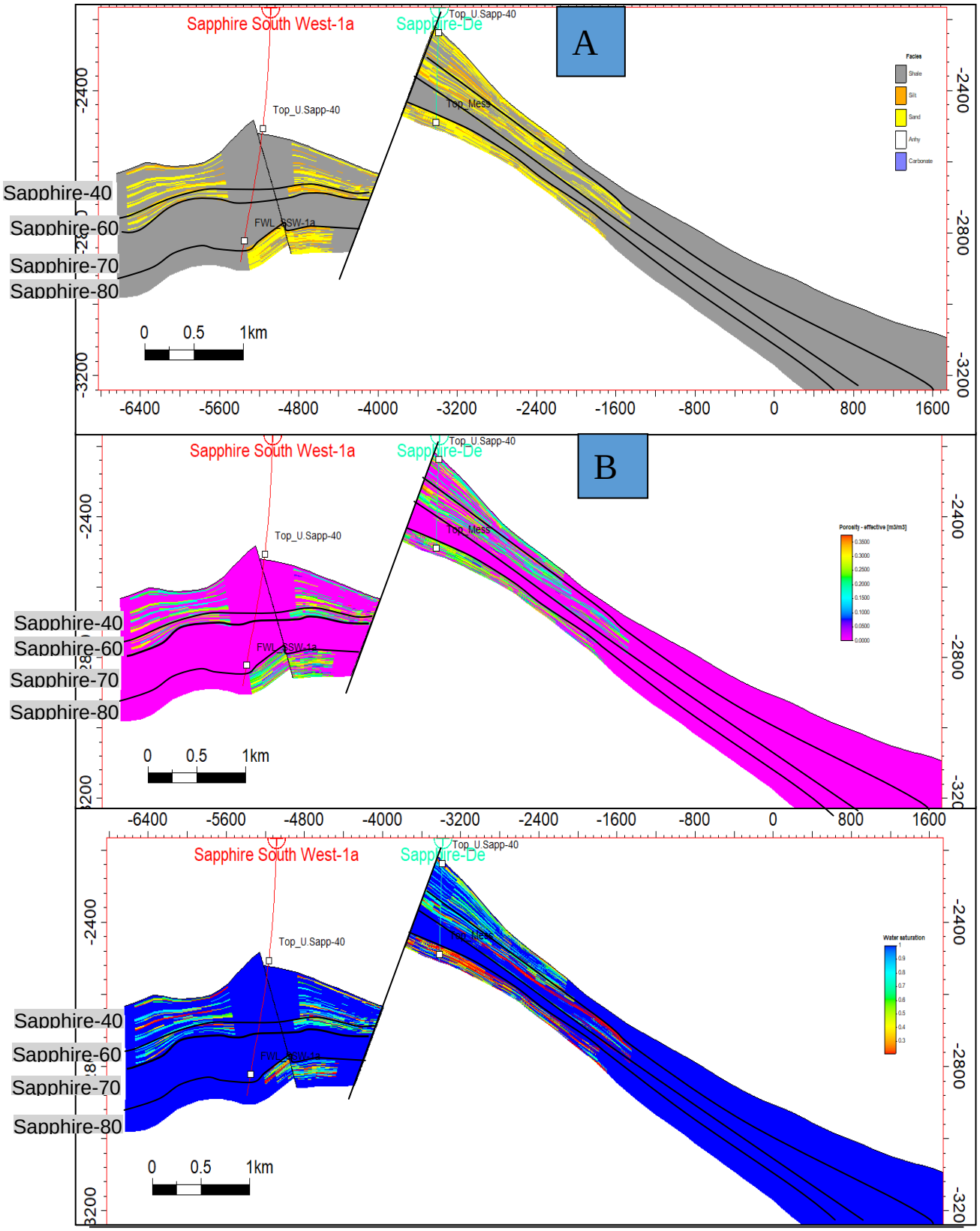

Fig. 19. North-south cross-section through the 3D model: (a) lithofacies, (b) effective porosity and (c) water

4. Prospectivity

As a result of the current study utilizing facies and petrophysical parameter distribution in three dimensions: important undrilled area (red area) figures (14c, 16c and 17c), located in upthrown side of the NDOA fault that is characterized by very good petrophysical characteristics and is hydrocarbon bearing.

5. Discussion

Sehim el, in 2002, studied the structural architecture and tectonic synthesis of the Rosetta province, west Nile Delta, and concluded that: The Rosetta-structural system comprises two superimposed fault systems. The old one is reflected through en echelon relay wrench-flowers of transpression and associated push-up folds; this tectonic cessation was synchronous with continuous thrusting and wrenching along the ENE-tectonic trends (e.g., West Delta Deep Marine). By the Early Pliocene, the old Rosetta-wrench related structures are overlapped by a superimposed extensional regime through a cycle of negative tectonic inversion. The Upper Early Pliocene is the time of tectonic termination of the ENE-trending wrench-related growth folds, and extension took place, producing extensional faults parallel to the axes of the wrench-related folds. This negative tectonic inversion was contemporaneous with the continuation of the extensional tectonics along the NW-trending Rosetta extensional faults.

In the present study: the lower Pliocene interval studied structurally by a 3D model, that rivaled the same structure setting mentioned by (Sehim el at 2002). also, the present work, studied the facies distribution and its petrophysical characteristics, and could divided the lower Pliocene into four channels: Sapphire-80, 70, 60 and Sapphire-40.

6. Conclusions

As a result of the data interpretation and building a 3D model of sapphire field with facies and petrophysical characteristics distribution: we concluded that lower Pliocene interval in sapphire field has a very good sand reservoir containing hydrocarbon, these channel reservoirs affected in its distribution way by set of faults affected the lower Pliocene of the area under investigation, as well as, from the current research we detected undrilled area that located in upthrown side of the NDOA fault that is characterized by very good petrophysical characteristics and is hydrocarbon bearing.

7. Recommendations

As result of the current study, we recommended to drill the prospected area (red colored area figures 14c, 16c and 17c), that is located within three way dip closure and characterized by very good petrophysical characteristics and containing hydrocarbon within Sapphire channels

4. References

Abdel-Fattah, M. I., Metwalli, F. I., &Mesilhi, E. S. I. (2018). Static reservoir modeling of the Bahariya reservoirs for the oilfields development in South Umbarka area, Western Desert, Egypt. Journal of African Earth Sciences, 138, 1–13.https://doi.org/10.1016/j.jafrearsci.2017.11.002

Abdel-Fattah, M., Dominik, W., Shendi, E., Gadallah, M., and Rashed, M. (2010). 3D integrated reservoir modeling for Upper Safa Gas Development in Obaiyed Field, Western Desert, Egypt. In 72nd EAGE conference and exhibition incorporating SPE EUROPEC, Spain, June 2010. https://doi.org/10.3997/2214-4609.201401358.

Abdel-maksoud, A., Amin, A. T., El-Habaak, G. H., &Ewida, H. F. (2019a). Facies and petrophysical modeling of the Upper Bahariya Member in Abu Gharadig oil and gas field, north Western Desert, Egypt. Journal of African Earth Sciences, 149(C), 503–516.https://doi.org/10.1016/j.jafrearsci.2018.09.011

Abu amarah, B. A., Nabawy, B. S., Shehata, A. M., Kassem, O. M., &Ghrefat, H. (2019). Integrated geological and petrophysical characterization of oligocene deep marine unconventional poor to tight sandstone gas reservoir. Marine and Petroleum Geology, 109, 868-885.https://doi.org/10.1016/j.marpetgeo.2019.06.037

Bryant, I. D., & Flint, S. S. (1993). Quantitative clastic reservoir geological modeling: Problems and perspectives. In S. S. Flint & I. D. Bryant (Eds.), The geological modeling of hydrocarbon reservoirs and outcrop analogues. International Association of

Sedimentologists Special Publication (Vol. 15: 3–20). Wiley.https://doi.org/10.1002/9781444303957.ch1.

Didier Dubois, Helene Fargier and Philippe Fortemps (2003): Fuzzy scheduling: Modelling flexible constraints vs. coping with incomplete knowledge, European Journal of Operational Research 147(2):231-252.https://doi.org/10.1016/S0377-2217(02)00558-1.

Farouk, S., Jain, S., Abd- Elazez, M., El Shennawy, T., & Shaker, F. (2021) High resolution Pliocene–Pleistocene calcareous nannofossil distribution and paleoenvironmental changes in the northwest Nile Delta, Egypt. Lethaia, https://doi. org/10.1111/let.12444.

May, P.R., 1991. The eastern meiterranian Mesozoic basin: evaluationoilhabitate AAPG (Am. Assoc. Pet. Geol.) Bull. 75, 1215-1232.https://doi.org/10.1306/0C9B2911-1710-11D7-8645000102C1865D.

Radwan, A. E. (2022). Chapter 2 Three-dimensional gas property geological modeling and simulation. In A. D. Wood & J. Cai (Eds.) Sustainable geoscience for natural gas sub-surface systems, Elsevier. pp. 29-45.https://doi.org/10.1016/B978-0-323-85465-8.00011-X.

Sehim, A., Hussein, M., Kasem, A., Shaker, A., &Swidan, N. (2002): Structural architecture and tectonic synthesis Rosetta Province, West Nile Delta Mediterranean. In Egypt, presented at Mediterranean offshore conference (MOC), Alexandria.

Wachowicz-et-al-2016: Methodology and results of digital mapping and 3D modelling of the Lower Palaeozoic strata on the East European Craton, Poland. https://doi.org/10.14241/asgp.2019.25.

نمذجة ثلاثية الأبعاد للخزان: دراسة لعصر البليوسين المبكر (متكون كفرالشيخ)، حقل غاز سافير، البحر المتوسط، مصر

أحمد إبراهيم أحمد أبو سلامة[١]، وعادل علي علي عثمان[٢]، فاروق إبراهيم متولي[٣]، ومحمد فتحي[٢]

[١] الهيئة المصرية العامة للبترول، مدينة نصر، القاهرة، مصر

[٢] قسم الجيولوجيا، كلية العلوم، جامعة الأزهر، القاهرة، مصر

[٣] قسم الجيولوجيا، كلية العلوم، جامعة حلوان، حلوان، مصر

يقع حقل غاز سافير في منطقة غرب الدلتا البحرية العميقة في مياه البحر المتوسط، مصر. والذي يحتوي على الوحدات الصخرية الحاملة للمواد الهيدروكربونية، وهى سافير ٤٠، إسفير-٦٠، سافير ٧٠، إسفير-٨٠ والتابعة لمتكون كفر الشيخ. وتهدف هذه الدراسة إلى بناء نموذج جيولوجي ثلاثي الأبعاد، والذي يمكننا من دراسة البناء التركيبي وتوزيع السحنات الصخرية والخصائص البتروفيزيائية لفهم توزيع خصائص الخزان، ولتحديد أماكن جديدة في حقل سافير. ومن خلال هذه الدراسة تم تقسيم القنوات الرملية التابعة لمتكون كفر الشيخ والتابع لعصر البليوسين السفلي من الأعلى إلى الأسفل إلى سافير ٤٠، إسفير-٦٠، سافير ٧٠، إسفير-٨٠، كما تم توزيع السحنات الصخرية والخصائص البتروفيزيائية فى البناء التركيبى للحقل. والذي من خلاله تم دراسة توزيع خصائص الخزان في منطقة الدراسة وبناء عليه تم تحديد بعض الأماكن لحفر آبار استكشافية وتنموية في المنطقة.